Published in final edited form as:

Sci Transl Med. 2013 October 16; 5(207): 207ra141. doi:10.1126/scitranslmed.3006479.

Inhibition of the Cardiomyocyte-Specific Kinase TNNI3K Limits Oxidative Stress, Injury, and Adverse Remodeling in the Ischemic Heart

Ronald J. Vagnozzi[1,2], **Gregory J. Gatto Jr.**[3], **Lara S. Kallander**[3], **Nicholas E. Hoffman**[2], **Karthik Mallilankaraman**[2], **Victoria L. T. Ballard**[3], **Brian G. Lawhorn**[3], **Patrick Stoy**[3], **Joanne Philp**[3], **Alan P. Graves**[4], **Yoshiro Naito**[5], **John J. Lepore**[3], **Erhe Gao**[2], **Muniswamy Madesh**[2], and **Thomas Force**[2,6,*]

[1]Program in Cell and Developmental Biology, Thomas Jefferson University, Philadelphia, PA 19107, USA

[2]Center for Translational Medicine, Temple University School of Medicine, Philadelphia, PA 19140, USA

[3]Heart Failure Discovery Performance Unit, Metabolic Pathways and Cardiovascular Therapeutic Area Unit, GlaxoSmithKline, King of Prussia, PA 19406, USA

[4]Platform Technology and Sciences, GlaxoSmithKline, King of Prussia, PA 19406, USA

[5]Cardiovascular Division, Department of Internal Medicine, Hyogo College of Medicine, Nishinomiya 663-8131, Japan

[6]Cardiology Division, Temple University School of Medicine, Philadelphia, PA 19140, USA

[*]Corresponding author. thomas.force@temple.edu.

SUPPLEMENTARY MATERIALS

www.sciencetranslationalmedicine.org/cgi/content/full/5/207/207ra141/DC1

Methods

Fig. S1. TNNI3K is localized to the cardiomyocyte nucleus.

Fig. S2. Basal LV function, hemodynamics, and cardiac morphometry in Tg-TNNI3K and Tg-KI TNNI3K mice.

Fig. S3. Post-I/R activation status of ERK1/2, JNK, and Akt in TNNI3K transgenic mice.

Fig. S4. Basal p38 MAPK activation status in TNNI3K transgenic mice.

Fig. S5. ERK1/2, JNK, and Akt activation status after *TNNI3K* overexpression in NRVMs.

Fig. S6. TNNI3K-induced cell death is blunted by selective knockdown of p38α in NRVMs.

Fig. S7. GSK854 rescues the effect of *TNNI3K* overexpression on ROS generation in NRVMs.

Fig. S8. *Tnni3k* deletion does not alter adverse LV remodeling after permanent occlusion MI.

Table S1. LV function and cardiac morphometry in inducible cardiomyocyte-specific *Tnni3k*-KO mice.

Table S2. Selectivity profiles of small-molecule TNNI3K inhibitors.

Author contributions: R.J.V. designed and performed the experiments, analyzed the data, and wrote the manuscript. G.J.G. analyzed the tissue-specific *Tnni3k* expression data. G.J.G. and L.S.K. led the GSK program team under the supervision of J.J.L. L.S.K., B.G.L., P.S., J.P., and A.P.G. discovered and supplied the TNNI3K inhibitor compounds. V.L.T.B. performed the biomarker analysis. N.E.H., K.M., and M.M. performed experiments and analyzed and interpreted data on mitochondrial function and ROS production. Y.N. provided materials and expertise on experiments in vivo. E.G. performed and provided expertise on all animal surgical procedures. G.J.G., L.S.K., J.J.L., and M.M. contributed to the final revision of the manuscript. T.F. designed the studies, interpreted and analyzed the data, and edited the manuscript.

Data and materials availability: The TNNI3K inhibitors described here may be shared upon reasonable request via a material transfer agreement with GSK.

Competing interests: Studies were funded in part by a grant from GSK (to T.F.). G.J.G., L.S.K., V.L.T.B., B.G.L., P.S., J.P., A.P.G., and J.J.L. are employees of GSK and have received compensation in the form of salary and stock. The use of TNNI3K inhibitors in cardiovascular disease is under patent WO2011088027.

Abstract

Percutaneous coronary intervention is first-line therapy for acute coronary syndromes (ACS) but can promote cardiomyocyte death and cardiac dysfunction via reperfusion injury, a phenomenon driven in large part by oxidative stress. Therapies to limit this progression have proven elusive, with no major classes of new agents since the development of anti-platelets/anti-thrombotics. We report that cardiac troponin I–interacting kinase (TNNI3K), a cardiomyocyte-specific kinase, promotes ischemia/reperfusion injury, oxidative stress, and myocyte death. TNNI3K-mediated injury occurs through increased mitochondrial superoxide production and impaired mitochondrial function and is largely dependent on p38 mitogen-activated protein kinase (MAPK) activation. We developed a series of small-molecule TNNI3K inhibitors that reduce mitochondrial-derived superoxide generation, p38 activation, and infarct size when delivered at reperfusion to mimic clinical intervention. TNNI3K inhibition also preserves cardiac function and limits chronic adverse remodeling. Our findings demonstrate that TNNI3K modulates reperfusion injury in the ischemic heart and is a tractable therapeutic target for ACS. Pharmacologic TNNI3K inhibition would be cardiac-selective, preventing potential adverse effects of systemic kinase inhibition.

INTRODUCTION

Overall patient prognosis and long-term survival after acute myocardial infarction (MI) largely depend on the extent of cardiomyocyte death during the primary ischemic event. Initial cardiomyocyte loss from ischemia is a critical phase of MI, which subsequently can contribute to arrhythmogenesis, adverse remodeling, and contractile dysfunction. For this reason, prompt restoration of coronary blood flow through percutaneous coronary intervention (PCI) is vital in preserving viable myocardium, and it remains a mainstay of care for patients with acute MI. However, PCI can also heighten loss of cardiomyocytes via a multifaceted process collectively termed “reperfusion injury” (1, 2). Upon coronary intervention, the rapid return of circulating oxygen and metabolites to compromised myocardium can drive reactive oxygen species (ROS) generation, intracellular Ca^{2+} overload, and up-regulation of proinflammatory molecules, ultimately triggering cell death in viable myocytes spared during ischemia. Reperfusion injury–induced pathologies have been purported to contribute markedly to post-MI infarct size (2, 3). Thus, although PCI is essential in limiting myocyte loss after MI, reperfusion injury is thought to diminish the maximum potential benefit of this intervention.

Despite the long-standing paradox of reperfusion injury, the underlying mechanisms driving cell death after ischemia remain undefined. Oxidative stress and mitochondrial dysfunction are major effectors, particularly in cardiomyocytes (4, 5). However, therapies to reduce oxidative stress and subsequent myocyte death during reperfusion of an acute MI have proven elusive. Therefore, new molecular players in the cardiomyocyte response to ischemia/reperfusion (I/R) injury and oxidative stress signaling must be identified. To this end, we began exploring the role of cardiac troponin I (cTnI)–interacting kinase (TNNI3K), also known as cardiac ankyrin repeat kinase (CARK). TNNI3K is a poorly understood protein kinase that appears to only be expressed in the heart.

TNNI3K was initially identified in fetal and adult human hearts but was undetectable in other tissues (6). Human *TNNI3K* encodes an 835–amino acid polypeptide with 10 ankyrin repeats, a central kinase domain, and a serine-rich C-terminal domain (6). TNNI3K autophosphorylates in vitro (7), but the functional consequences of this are unknown. cTnI was identified as a putative TNNI3K interaction partner from yeast two-hybrid screening, but whether cTnI is a direct biological target of TNNI3K is not known. Structural homology suggests that TNNI3K is a MAP3K [mitogen-activated protein kinase (MAPK) kinase kinase] superfamily member (6); however, no validated targets have been identified, and pathways regulated by TNNI3K remain unclear.

Little is known about the role of TNNI3K in cardiac biology. *TNNI3K* overexpression was reported to induce hypertrophy in neonatal rat ventricular myocytes (NRVMs) (8). Basal *Tnni3k* expression varied with genetic strain in mice, and higher-expressing strains progressed more rapidly to heart failure in the calsequestrin transgenic model of dilated cardiomyopathy (9). Furthermore, *TNNI3K* overexpression in DBA/2J mice, which have low endogenous levels, increased left ventricle (LV) dysfunction after pressure overload (9). Most recently, TNNI3K was reported to induce LV remodeling in mice in a kinase-dependent manner, but this was based solely on studies with considerable overexpression of wild-type or kinase-dead *TNNI3K* (10). Thus, TNNI3K may worsen heart failure progression in the setting of pressure overload, although this has yet to be confirmed with loss-of-function studies. TNNI3K has also been reported to regulate physiological hypertrophy, albeit also exclusively via overexpression approaches (11). The role of TNNI3K in I/R is largely undefined. One study reported improved LV function after injection of mouse embryonic carcinoma-derived (P19CL6) cells overexpressing *Tnni3k* into the border zone of infarcted hearts (12). However, these studies revealed little about the true biological roles of TNNI3K. Thus, much remains unknown about TNNI3K, and no studies have directly examined its role in the ischemic heart in vivo or the potential for modulating TNNI3K in human heart disease.

We used TNNI3K gain- and loss-of-function genetic mouse models, along with small-molecule TNNI3K inhibitors we developed, to examine the role of TNNI3K in the cardiomyocyte response to I/R injury. Inhibition of TNNI3K reduced infarct size, ROS levels, and p38 activation after I/R when delivered during reperfusion in mice. TNNI3K inhibition also limited chronic LV dysfunction and adverse remodeling in the mouse. The cardiac-restricted expression of TNNI3K suggests that on-target toxicity in other organs, which remains a major impediment to the clinical use of kinase inhibitors, would not occur with TNNI3K inhibition. In sum, our preclinical studies support TNNI3K as a viable target for acute coronary syndromes (ACS).

RESULTS

TNNI3K is a cardiomyocyte-specific protein kinase up-regulated in heart failure

To verify the cardiac-specific expression of *TNNI3K*, we used an mRNA panel from 64 nonpathological human tissues. TNNI3K was highly expressed in all heart chambers, more so in the ventricles than in the atria, and was virtually undetectable in all other tissues except the brain and testes (about 5% of that detected in heart) (Fig. 1A). We also measured

TNNI3K protein levels across a panel of murine tissues. TNNI3K was enriched in cardiomyocytes but was not detectable in cardiac fibroblasts, vascular endothelial cells, or skeletal muscle (Fig. 1B). Thus, TNNI3K appeared to be exclusive to the cardiomyocyte.

We performed subcellular fractionation studies in NRVMs and detected TNNI3K exclusively in the nuclear fraction (fig. S1A). Immunofluorescence staining showed TNNI3K enrichment around nuclei in both adult rat myocytes (fig. S1B) and NRVMs (fig. S1C). There was no colocalization with the actin-binding protein α-actinin basally or after oxidative or β-adrenergic stress, suggesting that it does not interact with cTnI, at least at the sarcomere. Finally, we measured TNNI3K levels in LV explants from ischemic cardiomyopathy (ICM) patients undergoing heart transplant. TNNI3K was significantly increased in hearts from ICM patients, versus nonfailing control hearts (Fig. 1C), suggesting that TNNI3K may play a role in human ischemic heart disease.

TNNI3K increases infarct size, ROS generation, and cardiomyocyte death in the ischemic heart

To characterize the role of TNNI3K in the ischemic heart in vivo, we generated cardiac-specific transgenic (Tg) mice on the FVB/N background, expressing human *TNNI3K* or a kinase-inactive (KI) TNNI3K point mutant, K490R (6). These mice showed a seven- to eightfold increase in TNNI3K protein versus nontransgenic littermates (wild type) (Fig. 2A). We saw no effects of either transgene on basal LV function, cardiac morphometry (fig. S2, A and B), or contractile function (fig. S2, C and D).

We induced I/R in these mice via coronary artery occlusion/release (13) and assessed infarct size after 24 hours. After I/R, infarcts were significantly larger in Tg-TNNI3K mice versus wild-type littermates (Fig. 2B), whereas areas at risk (AARs) did not differ (Fig. 2C). Further, Tg-TNNI3K mice had elevated plasma levels of cTnI, an indicator of cardiomyocyte death (Fig. 2D). Conversely, Tg-KI TNNI3K mice had significantly smaller infarcts than Tg-TNNI3K animals, as well as lower plasma cTnI levels, suggesting that increased TNNI3K kinase activity is detrimental in the setting of acute I/R.

One particularly crucial element of reperfusion injury in the heart is the elevation of ROS levels (4, 14, 15). Therefore, to assess the potential contribution of TNNI3K to post-I/R ROS generation, we performed ex vivo molecular detection of superoxide using the redox-sensitive compound dihydroethdium (DHE) (16). Hearts from Tg-TNNI3K mice showed significantly elevated basal superoxide versus those from wild-type littermates, as indicated by increased mean DHE intensity, as well as regions of punctate DHE staining, indicative of nuclear labeling (Fig. 2E). In contrast, there was no increase in basal superoxide in hearts from Tg-KI TNNI3K mice. Next, we examined post-I/R superoxide levels 30 min after reperfusion, when ROS generation has been shown to peak (15, 17). Although I/R significantly increased DHE intensity in all three groups, this effect was exacerbated in Tg-TNNI3K mice, which had greater DHE staining after I/R versus wild-type or Tg-KI TNNI3K animals (Fig. 2F). This suggests that TNNI3K promotes ROS generation in the heart after I/R injury.

TNNI3K induces mitochondria-derived ROS overproduction, mitochondrial dysfunction, and bioenergetic impairment in cardiomyocytes

Mitochondria are a major source of ROS in the heart, and oxidative stress due to mitochondrial dysfunction substantially contributes to reperfusion injury (18, 19). Given the elevation in ROS seen in TNNI3K transgenic mice, we asked whether TNNI3K modulates mitochondria-derived ROS (mROS) production. We overexpressed *TNNI3K* via adenoviral gene delivery in cultured NRVMs, and after 24 hours, the cells were loaded with the mitochondrial superoxide–sensitive indicator MitoSOX Red, and mROS were imaged by confocal microscopy. *TNNI3K* overexpression significantly increased MitoSOX Red oxidation in NRVMs, indicative of elevated superoxide production (Fig. 3A). Pretreatment with diphenyleneiodonium, which inhibits NAD(P)H oxidase–dependent cytosolic ROS production, did not alter this effect, whereas ectopic expression of mitochondrial superoxide dismutase (*MnSOD*/*SOD2*) abrogated the TNNI3K-induced overproduction of superoxide (Fig. 3A). These data indicate that mitochondria are the source of elevated superoxide after *TNNI3K* overexpression.

To assess whether TNNI3K-mediated mROS elevation alters mitochondrial function in cardiomyocytes, we simultaneously measured mitochondrial Ca^{2+} uptake and mitochondrial membrane potential ($\Delta\psi_m$) in permeabilized cardiomyocytes isolated from adult Tg-TNNI3K mice or wild-type littermates. Tg-TNNI3K myocytes had decreased basal $\Delta\psi_m$ versus wild type, as well as reduced calcium uptake into the mitochondria after sequential pulses of Ca^{2+} (Fig. 3B). When treated with the mitochondrial uncoupler carbonyl cyanide 3-chlorophenylhydrazone (CCCP), Tg-TNNI3K myocytes also showed a reduction in total Ca^{2+} release from mitochondria versus wild-type myocytes, consistent with decreased $\Delta\psi_m$ and an inability to clear extracellular Ca^{2+}. To confirm these findings in intact cells, we quantified tetramethyl rhodamine ethyl ester (TMRE) uptake in NRVMs after *TNNI3K* overexpression (Fig. 3C). Similar to our findings in permeabilized myocytes, cells overexpressing *TNNI3K* had significantly reduced TMRE fluorescence, indicative of reduced $\Delta\psi_m$.

Finally, we assessed the effect of TNNI3K on overall cellular bioenergetics by measuring oxygen consumption rate in NRVMs infected with TNNI3K adenovirus or a control green fluorescent protein (GFP) adenovirus. After basal oxygen consumption rate measurement, cells were sequentially challenged with an adenosine triphosphate (ATP) synthase inhibitor (oligomycin), followed by an ionophore [carbonyl cyanide 4-(trifluoromethoxy)phenylhydrazone (FCCP)] and, finally, electron transport chain inhibitors (antimycin A + rotenone). Collectively, these agents reveal the mitochondrial response to bioenergetic dysfunction owing to impaired ATP generation and $\Delta\psi_m$ disruption. *TNNI3K* overexpression altered the overall energetic profile in NRVMs (Fig. 3D), characterized by a significantly reduced basal oxygen consumption before challenge (Fig. 3E). Moreover, maximal respiration rate upon treatment with the uncoupling agent FCCP was significantly reduced in NRVMs overexpressing *TNNI3K* (Fig. 3F), suggesting that TNNI3K impairs mitochondrial bioenergetics and the ability of the cardiomyocyte to respond to energetic crisis. However, mitochondrial coupling efficiency upon oligomycin treatment was not altered by *TNNI3K* overexpression (Fig. 3G), indicating that TNNI3K does not directly

affect electron flow through the mitochondrial electron transport chain. Thus, TNNI3K augmented mitochondrial dysfunction in rodent cardiomyocytes by increasing superoxide levels, thereby reducing $\Delta\psi_m$ and impairing Ca^{2+} uptake capacity and bioenergetic output. In line with our ex vivo ROS detection studies, TNNI3K-dependent cardiomyocyte dysfunction occurs, at least in part, through mROS overproduction and subsequent mitochondrial impairment.

TNNI3K worsens ischemic injury and cardiomyocyte death via p38

Although structural homology suggests that TNNI3K is a MAP3K superfamily member (6), the signaling pathways downstream of TNNI3K are unknown. Thus, we examined activation of classical MAPK cascades in hearts from *TNNI3K* transgenic mice after I/R. *TNNI3K* but not KI *TNNI3K*, overexpression significantly increased p38 activation specifically in the ischemic LV, 3 hours after I/R (Fig. 4A). In contrast, no significant difference in extracellular signal–regulated kinase 1/2 (ERK1/2), c-Jun N-terminal kinase (JNK), or Akt pathway activation was detected (fig. S3). *TNNI3K* overexpression alone was not sufficient to induce p38 MAPK activation in vivo (fig. S4). Therefore, to determine if elevated p38 activation was truly due to TNNI3K activity, we infected NRVMs with myc-tagged *TNNI3K* adenovirus at increasing multiplicity of infection (MOI) or a GFP vector control and measured p38 phosphorylation. *TNNI3K* overexpression in NRVMs increased phosphorylation of p38 in a dose-dependent fashion (Fig. 4B), whereas ERK, JNK, and Akt activation were not observed (fig. S5), suggesting that TNNI3K specifically activates the p38 pathway in cardiomyocytes.

p38 is an established regulator of ROS generation and cell death in the heart. Therefore, we asked whether p38 inhibition suppresses the adverse effects of TNNI3K in the setting of I/R injury. We treated Tg-TNNI3K mice and wild-type littermates with a single dose of SB239063, a selective p38 inhibitor (20), and then subjected them to I/R. p38 inhibition abrogated the increased injury seen in Tg-TNNI3K animals, normalizing post-I/R infarct size to that of wild-type littermates (Fig. 4C). We also assessed the potential p38-mediated contribution of TNNI3K to cardiomyocyte death in the setting of simulated I/R. NRVMs overexpressing *TNNI3K* (at an MOI sufficient to activate p38; Fig. 4B) or GFP were exposed to hypoxic conditions (1% O_2) followed by reoxygenation (H/R). *TNNI3K* overexpression was sufficient to increase cardiomyocyte death versus GFP under normoxic conditions (Fig. 4D).

More striking, however, was the increase in post-H/R cell death with TNNI3K versus GFP (Fig. 4D). This effect was abolished by pretreatment with a ROS scavenger, suggesting that TNNI3K mediated cardiomyocyte death, in part, via ROS overproduction. Moreover, pretreatment with either of the two p38 inhibitors, each with different mechanisms of inhibition [SB239063 (21) or VX-702 (22)], blocked the effect of *TNNI3K* overexpression on cell death after H/R (Fig. 4D). Knockdown of p38α, but not p38β, blunted the TNNI3K-induced increase in myocyte death, implicating p38α as the predominant isoform activated downstream of TNNI3K (fig. S6).

Deletion of *Tnni3k* reduces infarct size, cardiomyocyte death, and p38 activation after I/R

Given the phenotype we observed with TNNI3K overexpression, we asked whether TNNI3K inhibition was protective in the setting of I/R. We first generated inducible *Tnni3k* knockout mice (*Tnni3k*-KO) via the α-MHC-Mer-Cre-Mer (MCM) system, which provided cardiomyocyte-restricted, tamoxifen-mediated deletion. We used C57BL/6 mice to study the effects of *Tnni3k* deletion in a background with moderately higher endogenous expression versus the strain used in the *TNNI3K* transgenics (9). TNNI3K protein in the LV was reduced by more than 90% in *Tnni3k*-KO mice compared with wild-type *Tnni3k*-floxed (fl/fl), MCM-negative (*Tnni3k*-competent) controls (Fig. 5A). Tamoxifen can induce cardiotoxicity in the Mer-Cre-Mer mouse (23), but we did not observe an effect on LV function or chamber dimensions with our protocol (table S1).

Tnni3k-KO and wild-type littermates were subjected to I/R as above. After 24 hours, *Tnni3k*-KO animals had significantly smaller infarcts (Fig. 5, B and C), yet AAR did not differ versus wild type (Fig. 5D). *Tnni3k*-KO animals also showed markedly reduced plasma levels of three injury biomarkers after I/R: cTnI, cardiac troponin T, and myosin light chain (Fig. 5E). Moreover, p38 activation was significantly reduced in *Tnni3k*-KO animals, whereas ERK1/2, JNK, and Akt activation were all unaltered (Fig. 5F), suggesting that the protection in these mice was due in part to reduced p38 activation. In contrast, *Tnni3k*-KO mice showed comparable LV dysfunction, hypertrophy, and adverse remodeling in a permanent occlusion model of MI without reperfusion (fig. S8). Thus, TNNI3K may specifically regulate the cardiomyocyte response to reperfusion injury.

TNNI3K inhibitors reduce superoxide production, p38 activation, and infarct size after I/R

TNNI3K loss of function appeared to be beneficial in the mouse heart after I/R. To translate this to the clinic, one would need to create inhibitors to deliver to patients. To this end, we developed two active site–binding small-molecule TNNI3K inhibitors: GSK329 and GSK854 (Fig. 6A). These inhibitors were highly potent and moderately selective (table S2). GSK329 does inhibit other kinases, including p38α [albeit to a limited extent (table S2)], but GSK854 has a unique selectivity profile versus GSK329 and no p38α-directed inhibition.

We asked whether TNNI3K inhibition confers any benefit when delivered after ischemia, at reperfusion, as a model of pharmacological intervention concomitant with PCI. Wild-type C57BL/6 mice were subjected to 30 min of ischemia and administered GSK329 or GSK854 via intraperitoneal injection at the time of reperfusion. TNNI3K inhibition significantly reduced infarct size versus vehicle control after I/R (Fig. 6, B and C), with no effect on AAR (Fig. 6D). Superoxide production in the ischemic LV 30 min after reperfusion was also blunted by TNNI3K inhibition (Fig. 6E). In the ischemic LV of GSK854-treated mice, there was a significant reduction in p38 phosphorylation with TNNI3K inhibition during reperfusion (Fig. 6F).

Finally, to directly assess the effects of TNNI3K inhibition on cellular stress and injury, we subjected isolated adult wild-type C57BL/6 mouse cardiomyocytes to H/R in the presence or absence of GSK854, and assessed $\Delta\psi_m$ maintenance. Thirty minutes after H/R, $\Delta\psi_m$ was significantly decreased in vehicle-treated myocytes, indicative of mitochondrial dysfunction

(Fig. 6G). Pretreatment with GSK854 before hypoxia blunted post-H/R $\Delta\psi_m$ impairment. Moreover, GSK854 also preserved $\Delta\psi_m$ after H/R when delivered during reoxygenation (Fig. 6H). In contrast, mitochondrial Ca^{2+} handling in the setting of H/R was not affected by TNNI3K inhibition after $\Delta\psi_m$ dissipation by CCCP, as indicated by equivalent total Ca^{2+} content levels (Fig. 6I).

TNNI3K inhibition seems to reduce mitochondrial dysfunction in isolated rodent cardiomyocytes exposed to simulated I/R, suggesting that the beneficial effects of in vivo TNNI3K inhibition are, at least in part, cardiomyocyte-autonomous. Of note, GSK854 also rescued the ROS elevation seen with TNNI3K overexpression in NRVMs (fig. S7), but did not alter ROS levels after treatment with antimycin A and ionomycin, which disrupt mitochondrial electron transport and lead to ROS production. Thus, GSK854 does not act as a non-specific ROS scavenger in cardiomyocytes.

TNNI3K inhibition reduces chronic LV dysfunction, progressive remodeling, and fibrosis in an ACS model

Although our TNNI3K inhibitors lessened infarct size and reduced ROS when delivered at reperfusion, we wanted to determine whether they could also confer long-term functional benefits after a more severe ischemic insult. Wild-type C57BL/6 mice were subjected to I/R, with an extended ischemic time of 40 min, to produce a reperfused myocardial infarction (MI/R). We intraperitoneally administered GSK854 immediately at reperfusion and again 6 hours after reperfusion. Animals were then given ad libitum access to chow containing GSK854 and followed for 6 weeks. Gross histological analysis of heart sections revealed a marked reduction in overall cardiac pathology with TNNI3K inhibition (Fig. 7A). Moreover, TNNI3K inhibition significantly ameliorated the decline in LV ejection fraction (%EF) seen at 2 weeks after MI/R (Fig. 7B). This functional benefit was maintained at 4 weeks after MI/R, as indicated by higher %EF (Fig. 7B) and smaller LV end-systolic dimension (Fig. 7C) versus vehicle-treated mice. Further, TNNI3K inhibition protected against adverse ventricular remodeling, as evidenced by a significantly smaller LV end-diastolic dimension at 4 weeks (Fig. 7D).

At 6 weeks after MI/R, heart failure progression was reduced by treatment with GSK854, as indicated by a marked decrease in plasma atrial naturetic peptide precursor (pro-ANP) levels compared with vehicle-treated animals (Fig. 7E). The increase in heart weight/body weight ratio after MI/R was slightly attenuated in inhibitor-treated animals (Fig. 7F, *P* value was not significant by one-way ANOVA). This suggests that TNNI3K inhibition might reduce pathological hypertrophy in this setting. Therefore, we also measured the cardiomyocyte cross-sectional area—a more sensitive measure of hypertrophy—and found significantly smaller myocytes in inhibitor-treated mice versus vehicle-treated mice after MI/R (Fig. 7G), confirming reduced cellular hypertrophy, which may account for the attenuation in heart weight/body weight ratio. Cardiac fibrosis at 6 weeks after MI/R was also reduced with TNNI3K inhibition (Fig. 7H).

DISCUSSION

Herein we report that TNNI3K, a cardiomyocyte-specific kinase, is a promoter of mROS production and p38 MAPK activation, which worsens I/R injury in the heart when overexpressed in mice. Cardiac-specific deletion or pharmacological inhibition of TNNI3K decreased ROS generation and p38 activation, protecting the heart from reperfusion injury and ultimately reducing infarct size and limiting adverse remodeling after MI in mice. The TNNI3K inhibitor described here could be delivered after ischemia, thus mimicking delivery upon PCI in ACS patients. Effective pharmacological agents that can afford protection when delivered after coronary reperfusion remain an unmet clinical need. Notably, previous trials of several classes of agents, including anti-inflammatories, statins, and erythropoietin, have failed to significantly improve long-term (or even short-term) clinical outcomes (1, 2). This has led to considerable efforts to target specific mechanisms of reperfusion injury, such as oxidative stress (24).

The potency of protection achieved through post-ischemia TNNI3K inhibition is consistent with the mitochondrial (Fig. 3, B and C) and energetic (Fig. 3D) dysfunction we see with increased TNNI3K activity. In particular, the increase in mROS via TNNI3K (Fig. 3A) suggests that TNNI3K inhibition may be particularly effective in modulating oxidative stress and ROS-mediated signaling underlying reperfusion injury. Thus, TNNI3K inhibition could represent a therapeutic strategy for ACS that directly targets cardiomyocyte death after reperfusion.

Deletion of TNNI3K reduced injury and myocyte loss after I/R in rodents, but we observed no protection in a permanent occlusion MI model. Although this finding seems contradictory to the acute protective effect of TNNI3K inhibition, numerous studies suggest that ROS-mediated mechanisms of injury act predominantly in acute I/R, and less so in chronic remodeling after permanent occlusion MI. Indeed, multiple models have shown large ROS induction upon reperfusion, whereas ischemia itself is characterized by relatively minor ROS elevation (4, 14). Our studies suggest that the downstream signaling and subsequent regulation of cell death by TNNI3K are particularly responsive to ROS. Further, our findings reveal that the intracellular mechanisms underlying TNNI3K-mediated cardiomyocyte cell death are at least partly through mitochondrial dysfunction. Our data also suggest that the actions of TNNI3K may be specific to the reperfusion phase of I/R, making TNNI3K inhibition a distinct therapeutic complement to potentially diminish lethal reperfusion injury during PCI.

When delivered before hypoxia or during reoxygenation, a TNNI3K inhibitor preserved mitochondrial membrane potential in cardiomyocytes after H/R. This appeared to occur independently of mitochondrial Ca^{2+} handling, as there was an elevation in total Ca^{2+} content after H/R, which was unaffected by TNNI3K inhibition. In contrast, basal mitochondrial Ca^{2+} uptake was impaired in TNNI3K transgenic mouse myocytes, albeit in the setting of a highly compromised $\Delta\psi_m$, consistent with mitochondrial ROS elevation. Thus, TNNI3K may play a role in controlling mROS generation independent of mitochondrial Ca^{2+} handling, but further studies will be necessary to distinguish ROS-mediated versus ROS-independent functional effects of TNNI3K on mitochondria.

We have also identified p38 MAPK as a key downstream effector of TNNI3K. Although TNNI3K inhibition lessened I/R injury partly by suppressing p38, the magnitude of protection was proportionately larger than the degree of p38 inhibition observed with TNNI3K deletion or inhibition. TNNI3K likely has additional downstream targets that we did not investigate here, inhibition of which contributes to reduced ischemic injury and remodeling. Although the role of p38 in the ischemic heart remains controversial (25), many studies of I/R have demonstrated the detrimental effects of p38 via increased cardiomyocyte death. In particular, p38 is highly responsive to the ROS elevation seen in I/R (26, 27). Correspondingly, p38 inhibitors are beneficial in numerous models (28, 29), but adverse on- and off-target effects have hampered clinical translation. To address this, recent p38 inhibitor trials propose partial inhibition of the kinase (28), potentially limiting or even precluding therapeutic benefits with more complete inhibition. p38 MAPKs are ubiquitously expressed and regulate numerous biological responses. In contrast, TNNI3K is cardiomyocyte-specific, which is rare among protein kinases. Inhibiting TNNI3K could therefore avoid potential adverse effects of systemic p38 inhibition. Moreover, TNNI3K inhibitors might be suitable for patients with other conditions that include an oxidative burden. In particular, TNNI3K inhibition might be particularly applicable to patients with chronic ICM, whose recurrent ischemic episodes are followed by restoration of flow, mimicking repeated bouts of I/R.

On the basis of our findings, we propose that TNNI3K represents a therapeutic target for ACS. However, our studies were limited to rodent models of coronary occlusion, which use a short ischemic time (30) and do not fully recapitulate the coronary anatomy, pathophysiology, or co-morbidity in human disease. To fully assess potential clinical translation, trials of TNNI3K inhibition in large animals, examining both short-term (infarct size and cTnI release) and long-term (survival, LV function, and hemodynamics) outcomes, are required. These studies will serve to determine whether TNNI3K inhibitors could have therapeutic application in acute and/or chronic coronary disease.

MATERIALS AND METHODS

Study design

The objective of our study was to determine the role of TNNI3K in ischemic injury and remodeling of the heart. We used gain- and loss-of-function genetic mouse models, along with small-molecule TNNI3K inhibitors in vivo, and cultured murine myocytes as in vitro models. We used the minimum number of animals required to perform sufficient statistical analysis (typically $n < 12$ per group). Predefined endpoints were selected on the basis of the pathogenesis of cardiac injury and remodeling in mice and were assessed by echocardiography, plasma biomarker measurement, and histopathology. We measured the effects of TNNI3K on mitochondrial function and oxidative stress in cells or tissues using fluorescent indicators assessed by spectrophotometry and confocal microscopy. Modulation of kinase signaling pathways was assessed via Western blotting of heart or cell lysates with phospho-specific antibodies. Groups were randomly assigned for all treatments or surgical procedures. Assessment of all outcomes was performed by an observer blinded to the conditions of the experiment.

Analysis of TNNI3K expression in human tissues

Human expression data, along with accompanying sample descriptions, were obtained from Gene Logic (Ocimum Biosolutions Inc.) in 2006 and later organized by sample type. The full Gene Logic database consists of about 10,000 samples over hundreds of tissue types and can be obtained at http://www.ocimumbio.com. Only those samples having normal pathology, as described by Gene Logic (http://www.ncbi.nlm.nih.gov/pubmed/17059591), were analyzed in this study. Values for cardiac expression were determined from the left atrium (n = 191), LV (n = 19), right atrium (n = 219), or right ventricle (n = 233) samples. Expression data for each sample had been determined using mRNA amplification protocols as recommended by Affymetrix Inc. and subsequent hybridization to the Affymetrix U133_plus2 chip. Data were subjected to reported quality control measures including minimal 5′/3′ ratios for ACTB and GAPDH, as well as maximal scale factors as reported by Affymetrix MAS 5.0. Expression data were normalized using MAS 5.0 with a target intensity of 150.

Analysis of TNNI3K in human heart failure

Human left ventricular myocardium was obtained at the University of Pittsburgh from subjects with end-stage heart failure undergoing heart transplant or from organ donors whose hearts were unsuitable for donation owing to blood type, age, or size incompatibility. Transplant recipients had heart failure secondary to ICM. The nonfailing hearts from the organ donors demonstrated normal left ventricular function by echocardiography. Tissue aliquots were removed from the left ventricular free wall, rapidly frozen in liquid nitrogen, and stored at −70°C. The University of Pittsburgh Institutional Review Board approved the study, and consent was obtained from all subjects.

Mouse model of I/R injury

Ischemia was induced in TNNI3K transgenic or KO mice, littermate controls, or wild-type C57BL/6 mice (Jackson Laboratories) using left anterior descending (LAD) coronary artery occlusion under 2 to 2.5% inhaled isoflurane anesthesia, as described previously (13). After 30 or 40 min of ischemia, as indicated, the occlusion was released and animals were allowed to recover for the time indicated in each experiment. To determine the region at risk, 2% Evans blue dye was injected into the LV and allowed to circulate uniformly just before sacrifice. At the time of sacrifice, hearts were arrested in diastole by KCl cardioplegia solution injection, excised, sliced into 2-mm-thick sections, and placed in 2% TTC for 30 min. Sections were digitally photographed, and infarct region and AAR were quantified with SigmaScan Pro 5.0. All studies were conducted after review by the Institutional Animal Care and Use Committees of Thomas Jefferson University (TJU), Temple University School of Medicine (TUSM), and GlaxoSmithKline (GSK) and in accordance with the TJU, TUSM, and GSK Policies on the Care, Welfare, and Treatment of Laboratory Animals.

Administration of TNNI3K inhibitors or SB239063 in vivo

The discovery and synthesis of the TNNI3K inhibitors GSK329 and GSK854 are described in patent assay WO 2011/088027A1, available at: http://www.wipo.int/patentscope/search/en/WO2011088027. For intraperitoneal delivery of GSK329 or GSK854, the drug

was prepared from powder in a commercial solution of 20% aqueous Cavitron (hydroxypropyl-β-cyclodextrin) + 5% DMSO and administered at a final concentration of 2.75 mg/kg. This dose was based on PK/PD data for GSK854, roughly approximating the 100 mg/kg chow dosing in plasma level of inhibitor. To deliver GSK854 via chow, a small amount of powdered chow (PicoLab Rodent Diet 20, #5053, LabDiet) was twice mixed with the drug (powdered preparation) with a mortar and pestle. Contents of the mortar were added to remaining diet in a plastic bag and mixed on a rotator for 15 min. Animals were given ad libitum access to chow using glass feeder jars for the time(s) indicated. SB239063 was prepared from powder in a solution of Cremophor EL and administered at a dose of 15 mg/kg by oral gavage 1 hour before surgery.

Cell culture and analysis

Isolation of murine cardiomyocytes and calcium uptake, mitochondrial membrane potential ($\Delta\psi_m$), mitochondrial ROS, oxygen consumption rate, and cell death assays are described in Supplementary Methods.

Hypoxia/reoxygenation of isolated cardiomyocytes

Adult cardiac myocytes or NRVMs were incubated in Krebs buffer supplemented with 5 μM pyruvate and 50 μM sodium sulfite and placed in a cell culture incubator heated to 37°C and held at 1% O_2, 5% CO_2 for 30 min (adult myocyte experiments) or 2 hours (NRVM experiments). Cells were then changed to fresh culture medium and incubated under normoxic conditions at 37°C and 5% CO_2 for 30 min (adult myocytes) or 18 hours (NRVMs).

Statistical analysis

Significance between two groups was performed where indicated by Student's two-tailed *t* test with GraphPad Prism 5.0.1. In all other cases, significance across more than two groups was done in Prism with one-way ANOVA followed by Tukey's post hoc test. $P < 0.05$ was considered significant for all tests. Equal variance was assumed for all groups. All data are displayed as means ± SEM, unless otherwise noted.

Supplementary Material

Refer to Web version on PubMed Central for supplementary material.

Acknowledgments

We thank X. Shang, J. Song, and J. Yu for excellent technical assistance and M. Harpel, R. Willette, and D. Sprecher for critical reading of the manuscript.

Funding: This work was supported by an American Heart Association predoctoral fellowship (to R.J.V.), grants from the National Heart, Lung, and Blood Institute (HL-061688, HL-091799, and HL-106380 to T.F. and HL-086699 to M.M.), and a Shared Instrumentation Program grant (1S10RR027327 to M.M.). This work was also supported by the Scarperi family (to T.F.).

REFERENCES AND NOTES

1. Hausenloy DJ, Yellon DM. Myocardial ischemia-reperfusion injury: A neglected therapeutic target. J Clin Invest. 2013; 123:92–100. [PubMed: 23281415]
2. Yellon DM, Hausenloy DJ. Myocardial reperfusion injury. N Engl J Med. 2007; 357:1121–1135. [PubMed: 17855673]
3. Turer AT, Hill JA. Pathogenesis of myocardial ischemia-reperfusion injury and rationale for therapy. Am J Cardiol. 2010; 106:360–368. [PubMed: 20643246]
4. Murphy E, Steenbergen C. Mechanisms underlying acute protection from cardiac ischemia-reperfusion injury. Physiol Rev. 2008; 88:581–609. [PubMed: 18391174]
5. Baines CP. How and when do myocytes die during ischemia and reperfusion: The late phase. J Cardiovasc Pharmacol Ther. 2011; 16:239–243. [PubMed: 21821522]
6. Zhao Y, Meng XM, Wei YJ, Zhao XW, Liu DQ, Cao HQ, Liew CC, Ding JF. Cloning and characterization of a novel cardiac-specific kinase that interacts specifically with cardiac troponin I. J Mol Med. 2003; 81:297–304. [PubMed: 12721663]
7. Feng Y, Cao HQ, Liu Z, Ding JF, Meng XM. Identification of the dual specificity and the functional domains of the cardiac-specific protein kinase TNNI3K. Gen Physiol Biophys. 2007; 26:104–109. [PubMed: 17660584]
8. Wang L, Wang H, Ye J, Xu RX, Song L, Shi N, Zhang YW, Chen X, Meng XM. Adenovirus-mediated overexpression of cardiac troponin I-interacting kinase promotes cardiomyocyte hypertrophy. Clin Exp Pharmacol Physiol. 2011; 38:278–284. [PubMed: 21314842]
9. Wheeler FC, Tang H, Marks OA, Hadnott TN, Chu PL, Mao L, Rockman HA, Marchuk DA. *Tnni3k* modifies disease progression in murine models of cardiomyopathy. PLoS Genet. 2009; 5:e1000647. [PubMed: 19763165]
10. Tang H, Xiao K, Mao L, Rockman HA, Marchuk DA. Overexpression of TNNI3K, a cardiac-specific MAPKKK, promotes cardiac dysfunction. J Mol Cell Cardiol. 2013; 54:101–111. [PubMed: 23085512]
11. Wang X, Wang J, Su M, Wang C, Chen J, Wang H, Song L, Zou Y, Zhang L, Zhang Y, Hui R. TNNI3K, a cardiac-specific kinase, promotes physiological cardiac hypertrophy in transgenic mice. PLoS One. 2013; 8:e58570. [PubMed: 23472207]
12. Lai ZF, Chen YZ, Feng LP, Meng XM, Ding JF, Wang LY, Ye J, Li P, Cheng XS, Kitamoto Y, Monzen K, Komuro I, Sakaguchi N, Kim-Mitsuyama S. Overexpression of TNNI3K, a cardiac-specific MAP kinase, promotes P19CL6-derived cardiac myogenesis and prevents myocardial infarction-induced injury. Am J Physiol Heart Circ Physiol. 2008; 295:H708–H716. [PubMed: 18552163]
13. Gao E, Lei YH, Shang X, Huang ZM, Zuo L, Boucher M, Fan Q, Chuprun JK, Ma XL, Koch WJ. A novel and efficient model of coronary artery ligation and myocardial infarction in the mouse. Circ Res. 2010; 107:1445–1453. [PubMed: 20966393]
14. Lefer DJ, Granger DN. Oxidative stress and cardiac disease. Am J Med. 2000; 109:315–323. [PubMed: 10996583]
15. Becker LB. New concepts in reactive oxygen species and cardiovascular reperfusion physiology. Cardiovasc Res. 2004; 61:461–470. [PubMed: 14962477]
16. Cheng Z, Jiang X, Kruger WD, Praticò D, Gupta S, Mallilankaraman K, Madesh M, Schafer AI, Durante W, Yang X, Wang H. Hyperhomocysteinemia impairs endothelium-derived hyperpolarizing factor–mediated vasorelaxation in transgenic cystathionine β synthase–deficient mice. Blood. 2011; 118:1998–2006. [PubMed: 21653942]
17. Vanden Hoek TL, Li C, Shao Z, Schumacker PT, Becker LB. Significant levels of oxidants are generated by isolated cardiomyocytes during ischemia prior to reperfusion. J Mol Cell Cardiol. 1997; 29:2571–2583. [PubMed: 9299379]
18. Weiss JN, Korge P, Honda HM, Ping P. Role of the mitochondrial permeability transition in myocardial disease. Circ Res. 2003; 93:292–301. [PubMed: 12933700]
19. Baines CP. The mitochondrial permeability transition pore and ischemia-reperfusion injury. Basic Res Cardiol. 2009; 104:181–188. [PubMed: 19242640]

20. Johns DG, Ao Z, Willette RN, Macphee CH, Douglas SA. Role of p38 MAP kinase in postcapillary venule leukocyte adhesion induced by ischemia/reperfusion injury. Pharmacol Res. 2005; 51:463–471. [PubMed: 15749461]
21. Behr TM, Nerurkar SS, Nelson AH, Coatney RW, Woods TN, Sulpizio A, Chandra S, Brooks DP, Kumar S, Lee JC, Ohlstein EH, Angermann CE, Adams JL, Sisko J, Sackner-Bernstein JD, Willette RN. Hypertensive end-organ damage and premature mortality are p38 mitogen-activated protein kinase–dependent in a rat model of cardiac hypertrophy and dysfunction. Circulation. 2001; 104:1292–1298. [PubMed: 11551882]
22. Shao Z, Bhattacharya K, Hsich E, Park L, Walters B, Germann U, Wang YM, Kyriakis J, Mohanlal R, Kuida K, Namchuk M, Salituro F, Yao YM, Hou WM, Chen X, Aronovitz M, Tsichlis PN, Bhattacharya S, Force T, Kilter H. c-Jun N-terminal kinases mediate reactivation of Akt and cardiomyocyte survival after hypoxic injury in vitro and in vivo. Circ Res. 2006; 98:111–118. [PubMed: 16306447]
23. Koitabashi N, Bedja D, Zaiman AL, Pinto YM, Zhang M, Gabrielson KL, Takimoto E, Kass DA. Avoidance of transient cardiomyopathy in cardiomyocyte-targeted tamoxifen-induced MerCreMer gene deletion models. Circ Res. 2009; 105:12–15. [PubMed: 19520971]
24. Schwartz Longacre L, Kloner RA, Arai AE, Baines CP, Bolli R, Braunwald E, Downey J, Gibbons RJ, Gottlieb RA, Heusch G, Jennings RB, Lefer DJ, Mentzer RM, Murphy E, Ovize M, Ping P, Przyklenk K, Sack MN, Vander Heide RS, Vinten-Johansen J, Yellon DM. National Heart, Lung, and Blood Institute, National Institutes of Health, New horizons in cardioprotection: Recommendations from the 2010 National Heart, Lung, and Blood Institute Workshop. Circulation. 2011; 124:1172–1179. [PubMed: 21900096]
25. Rose BA, Force T, Wang Y. Mitogen-activated protein kinase signaling in the heart: Angels versus demons in a heart-breaking tale. Physiol Rev. 2010; 90:1507–1546. [PubMed: 20959622]
26. Clerk A, Fuller SJ, Michael A, Sugden PH. Stimulation of “stress-regulated” mitogen-activated protein kinases (stress-activated protein kinases/c-Jun N-terminal kinases and p38-mitogen-activated protein kinases) in perfused rat hearts by oxidative and other stresses. J Biol Chem. 1998; 273:7228–7234. [PubMed: 9516415]
27. Kulisz A, Chen N, Chandel NS, Shao Z, Schumacker PT. Mitochondrial ROS initiate phosphorylation of p38 MAP kinase during hypoxia in cardiomyocytes. Am J Physiol Lung Cell Mol Physiol. 2002; 282:L1324–L1329. [PubMed: 12003789]
28. Denise Martin E, De Nicola GF, Marber MS. New therapeutic targets in cardiology: p38 α mitogen-activated protein kinase for ischemic heart disease. Circulation. 2012; 126:357–368. [PubMed: 22801653]
29. Marber MS, Molkentin JD, Force T. Developing small molecules to inhibit kinases unkind to the heart: p38 MAPK as a case in point. Drug Discov Today Dis Mech. 2010; 7:e123–e127. [PubMed: 21278838]
30. Houser SR, Margulies KB, Murphy AM, Spinale FG, Francis GS, Prabhu SD, Rockman HA, Kass DA, Molkentin JD, Sussman MA, Koch WJ. American Heart Association Council on Basic Cardiovascular Sciences, Council on Clinical Cardiology, and Council on Functional Genomics and Translational Biology. Animal models of heart failure: A scientific statement from the American Heart Association. Circ Res. 2012; 111:131–150. [PubMed: 22595296]

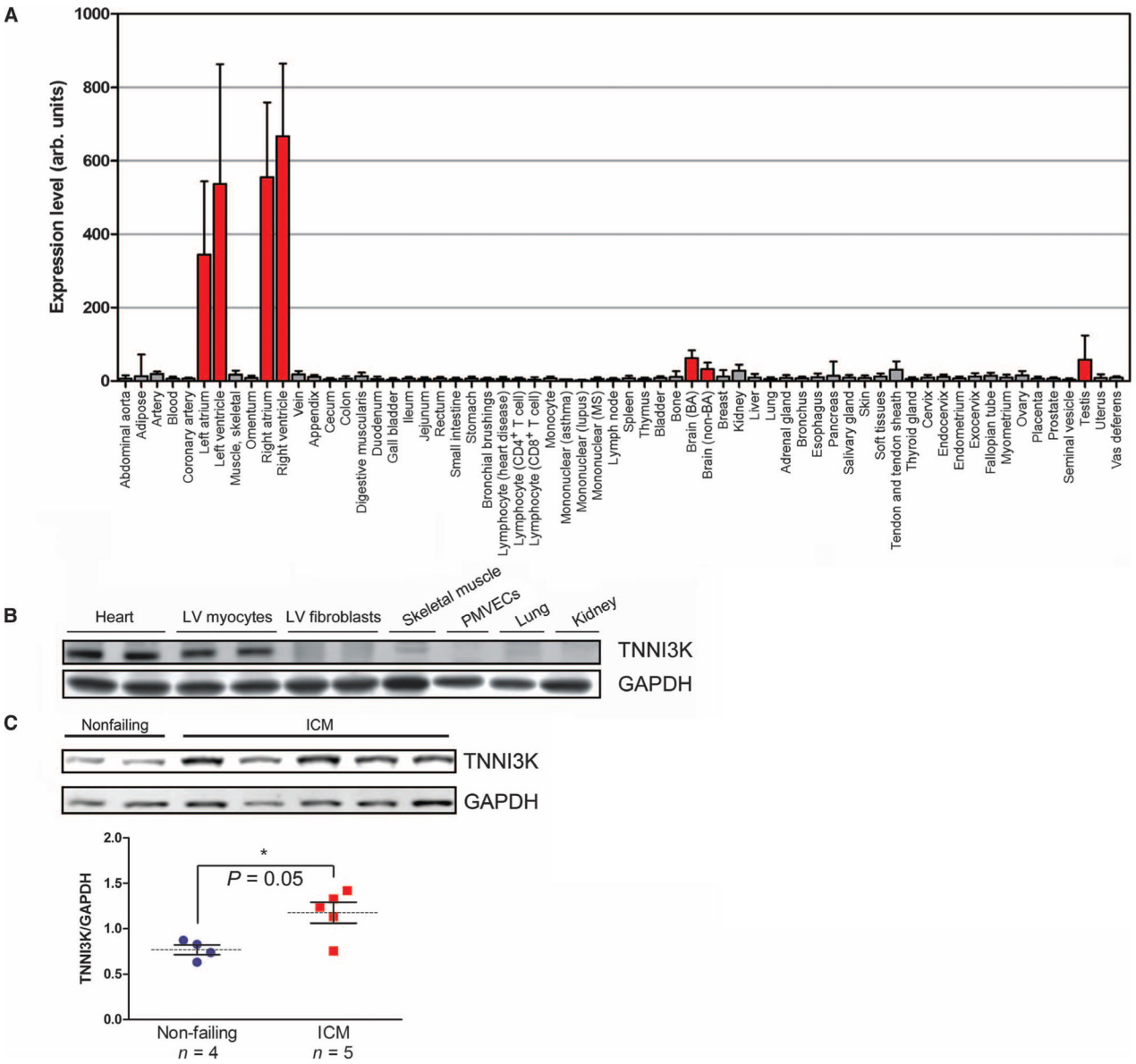

Fig. 1. *TNNI3K* is expressed in cardiomyocytes and is up-regulated in human heart failure

(**A**) *TNNI3K* transcript levels detected across a panel of primary non-pathological human tissue samples. (**B**) TNNI3K protein level as assessed by Western blot in lysates from whole heart, isolated myocytes, or fibroblasts of the LV; skeletal muscle; peripheral microvascular endothelial cells (PMVECs); lung; or kidney from adult C57BL/6 mice. Glyceraldehyde-3-phosphate dehydrogenase (GAPDH) served as a loading control for total protein level. (**C**) TNNI3K protein level as assessed by Western blot in LV explants from failing hearts of ICM patients undergoing transplant, or nonfailing controls. Data are shown as individual values with means (dashed lines) ± SEM (vertical bars) displayed. **P* value determined by Student's two-tailed *t* test.

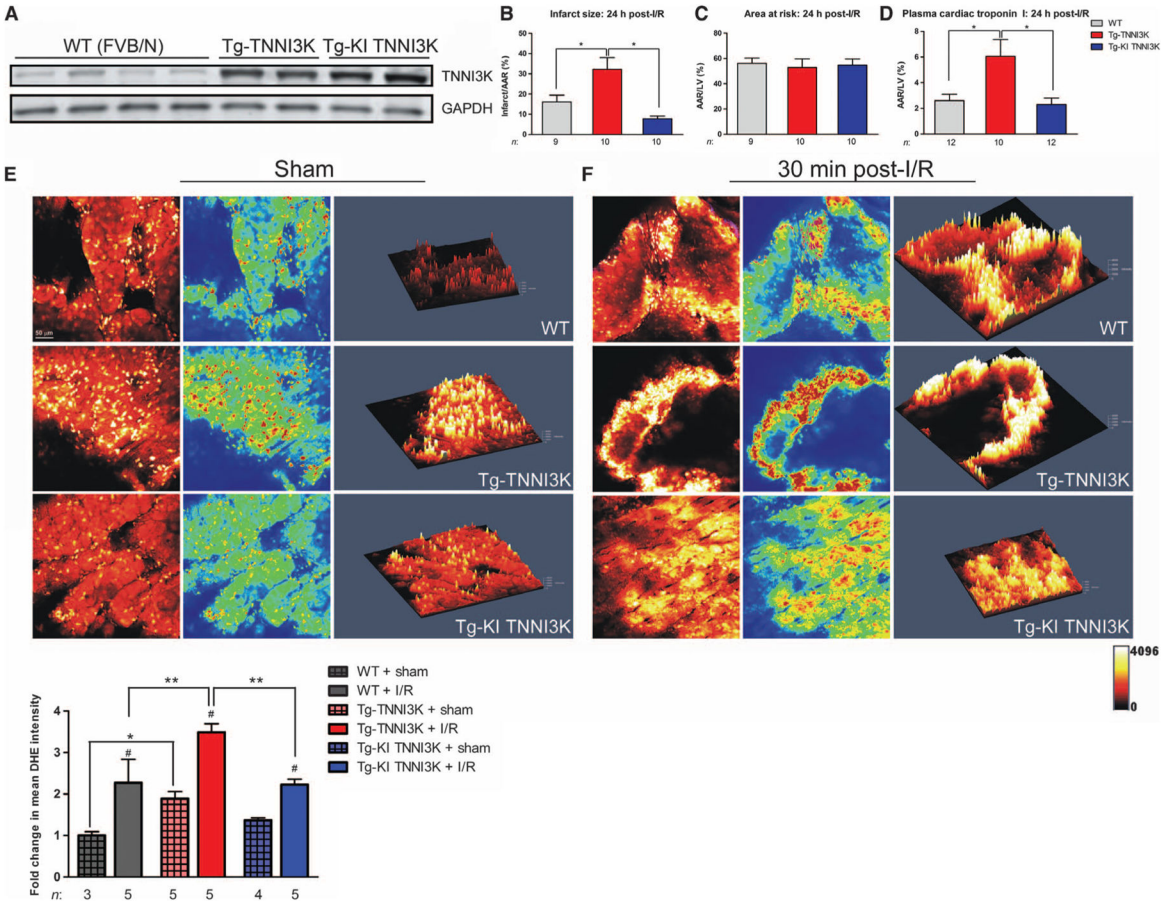

Fig. 2. *TNNI3K* overexpression increases infarct size, myocyte loss, and ROS production in mice after I/R

(**A**) TNNI3K protein level as measured by Western blot in LV lysates from Tg-*TNNI3K* or KI point-mutant (K490R) *TNNI3K* mice. Control animals were nontransgenic littermates [wild type (WT)]. GAPDH served as a loading control. (**B**) Infarct size 24 hours after I/R in Tg-TNNI3K ($n = 10$) or Tg-KI TNNI3K mice ($n = 10$), measured as a percentage of LV AAR. WT animals served as controls ($n = 9$). (**C** and **D**) AAR, measured as a percentage of total LV area (C), and plasma levels of cTnI (D) in the same groups as in (B), 24 hours after I/R. (**E** and **F**) Cardiac superoxide levels as measured by DHE staining of LV tissue from Tg-TNNI3K or Tg-KI TNNI3K mice after sham surgery (E) or 30 min after I/R (F). Confocal micrographs, heat-mapped versions, and Z-stack–generated 2.5-dimensional reconstructions from each condition are shown. Quantification is shown below representative images ($n = 3$ to 5 animals per group, as indicated). $^{*}P < 0.05$, $^{**}P < 0.01$, one-way analysis of variance (ANOVA) followed by Tukey's post hoc test. $^{\#}P < 0.05$ between post-I/R and sham conditions in each genotype.

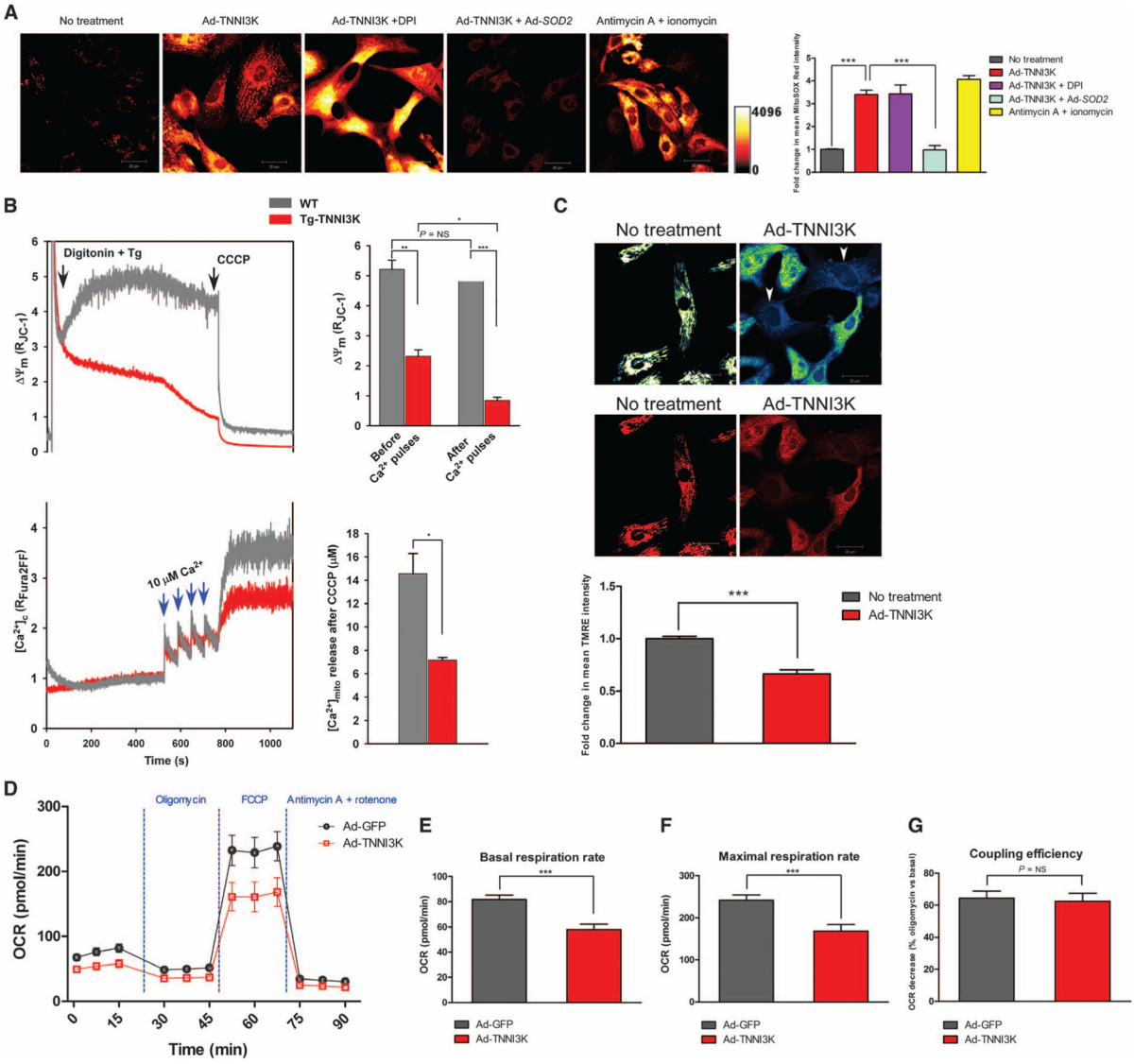

Fig. 3. TNNI3K increases mROS, impairs mitochondrial function, and decreases cellular bioenergetics in rodent cardiomyocytes

(**A**) Representative confocal micrographs from *n* = 3 biological replicates of NRVMs loaded with MitoSOX Red. Cells were infected with Ad-*TNNI3K* or Ad-*TNNI3K* + Ad-*SOD2* for 24 hours before imaging. NRVMs were challenged with diphenyleneiodonium (DPI) or antimycin A + ionomycin. Quantification of fold change in fluorescence is shown. (**B**) Representative mitochondrial membrane potential ($\Delta\psi_m$) and Ca^{2+} uptake traces in freshly isolated, permeabilized cardiomyocytes from WT and Tg-TNNI3K mice (*n* = 3 animals per group). Quantified changes in $\Delta\psi_m$ and bath [Ca^{2+}] due to mitochondrial Ca^{2+} uptake, in response to four pulses of Ca^{2+}, are shown. (**C**) Representative confocal micrographs from *n* = 3 biological replicates of intact NRVMs loaded with the $\Delta\psi_m$ indicator TMRE and imaged by confocal microscopy. Heat-mapped (top) and fluorescence (bottom) images with or without *TNNI3K* overexpression are shown. Arrowheads indicate cells with reduced TMRE uptake. Quantification of fold change in TMRE fluorescence is shown. (**D**) Oxygen

consumption rates (OCR) in intact NRVMs (n = 12 biological replicates per group), 24 hours after infection with Ad-TNNI3K or Ad-GFP (control). Cells were sequentially stimulated with oligomycin, FCCP, and antimycin A + rotenone. (**E** to **G**) Quantification of basal OCR before stimulation (E), maximal OCR after FCCP (F), and coupling efficiency (G) from the experiment described in (D). For all graphs, data are shown as means ± SEM. *P < 0.05, **P < 0.01, ***P < 0.001 as determined by two-tailed t test (B) or one-way ANOVA followed by Tukey's post hoc test (A and C to G).

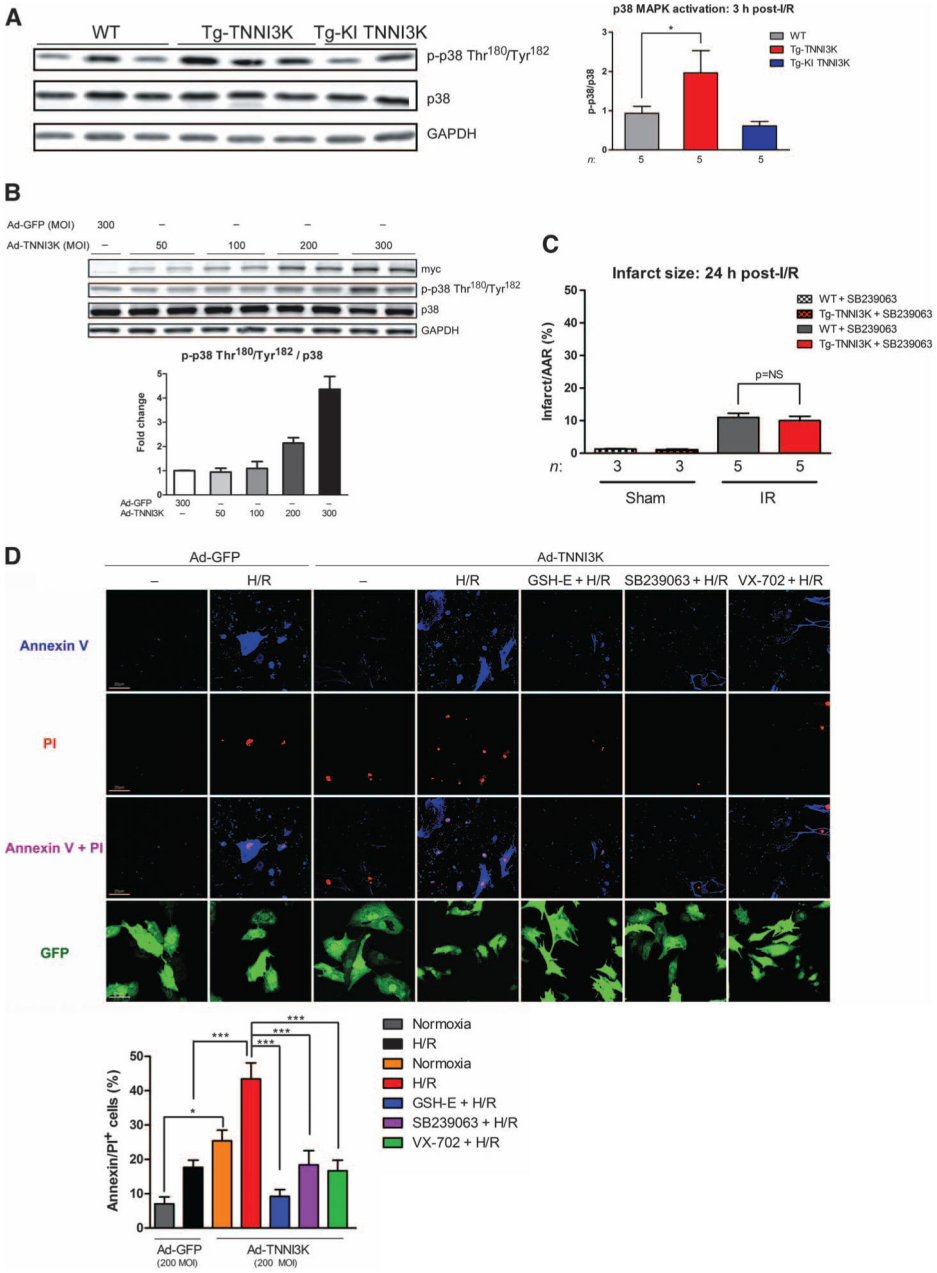

Fig. 4. TNNI3K promotes I/R injury and cardiomyocyte death through increased p38 MAPK activation

(**A**) Levels of phosphorylated and total p38 MAPK in lysates from the ischemic LV of Tg-TNNI3K or Tg-KI TNNI3K mice, 3 hours after I/R. GAPDH served as a loading control for total protein. Quantification from *n* = 5 animals per group is shown. (**B**) Levels of phosphorylated and total p38 MAPK in lysates from NRVMs infected with increasing MOI of adenoviruses expressing either N-terminal myc-tagged TNNI3K or GFP. Levels of myc epitope served as an indicator of *TNNI3K* overexpression, and GAPDH was a loading control. Quantification from *n* = 3 biological replicates is shown below the immunoblots. (**C**) Infarct sizes 24 hours after I/R in Tg-TNNI3K or WT mice treated with the p38 inhibitor

SB239063 1 hour before I/R. (**D**) Representative confocal micrographs from $n = 3$ biological replicates of intact NRVMs labeled with propidium iodide (PI) and annexin V, after H/R. Cells were infected with Ad-*TNNI3K* or Ad-GFP control 24 hours before H/R. Cells were treated with glutathione ester (GSH-E) or SB239063 or VX-702 1 hour before H/R. Scale bars, 20 μm. Quantification of cell death (as percent of PI^+/annexin V^+ cells) is shown. For all graphs, data are means ± SEM. *$P < 0.05$, ***$P < 0.001$ as determined by one-way ANOVA followed by Tukey's post hoc test.

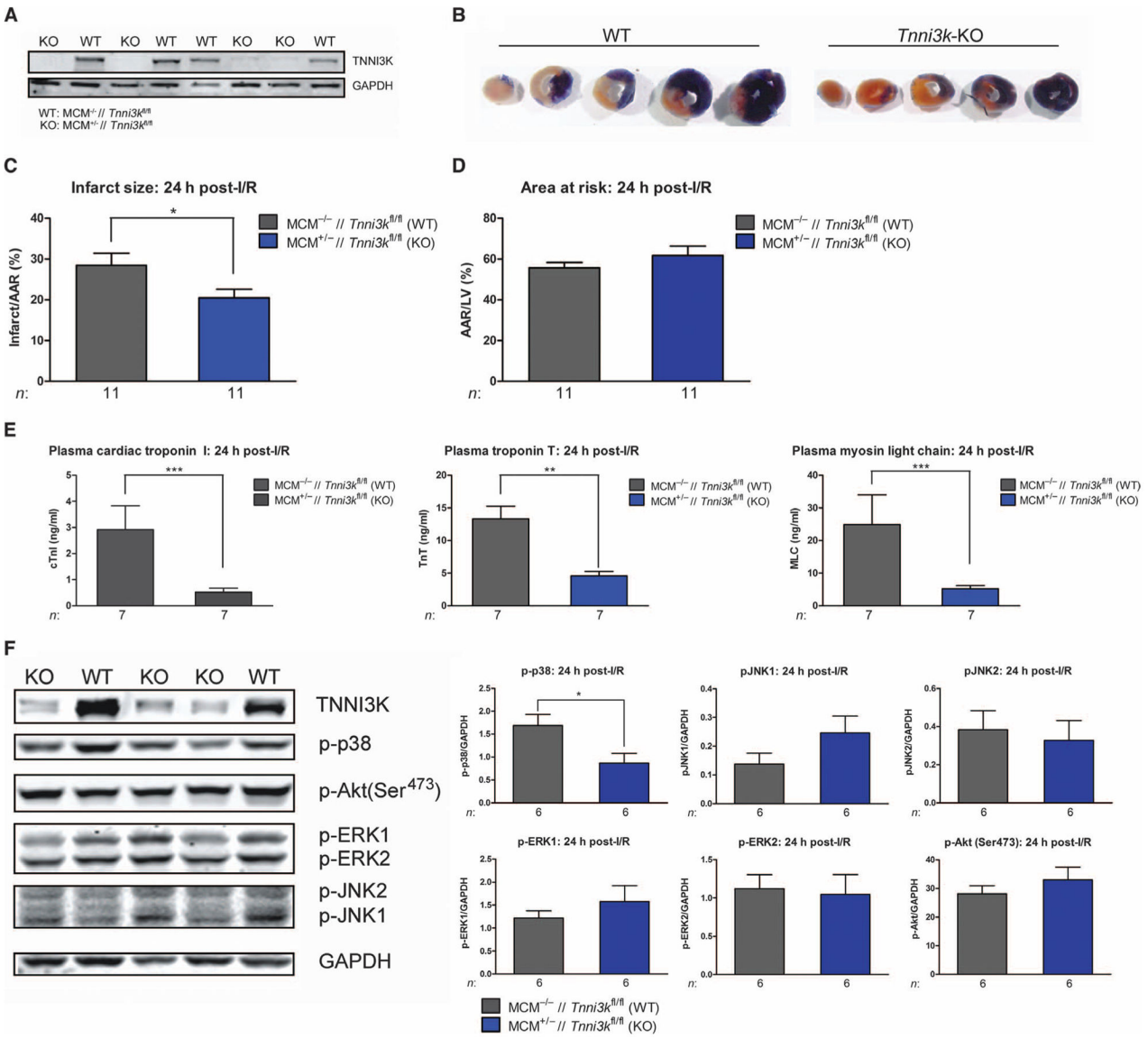

Fig. 5. Deletion of *Tnni3k* reduces infarct size, cardiomyocyte loss, and p38 MAPK activation after I/R

(**A**) TNNI3K protein levels in the LV of inducible cardiomyocyte-specific *Tnni3k*-KO mice or *Tnni3k*-floxed (fl/fl), Mer-Cre-Mer–negative ($MCM^{-/-}$) WT littermate controls, 5 days after the final dose of tamoxifen. (**B**) Representative Evans blue– and triphenyltetrazolium chloride (TTC)–stained LV sections from *Tnni3k*-KO mice or WT controls ($n = 11$ per group). (**C**) Infarct sizes as a percentage of the AAR. (**D**) AAR per total LV. (**E**) Plasma levels of cTnI, plasma troponin T (cTnT), and myosin light chain (MLC). (**F**) Representative continuous immunoblots ($n = 6$ animals per group) for phosphorylation status of Akt, ERK1/2, JNK1/2, or p38 MAPK in the remote LV of *Tnni3k*-KO or WT mice. TNNI3K and GAPDH are shown as controls. Quantification is shown on the right. All measurements in (B) to (F) were made 24 hours after I/R. All data in (C) to (F) are means ± SEM. $^{*}P < 0.05$, $^{**}P < 0.01$, $^{***}P < 0.001$, two-tailed Student's *t* test.

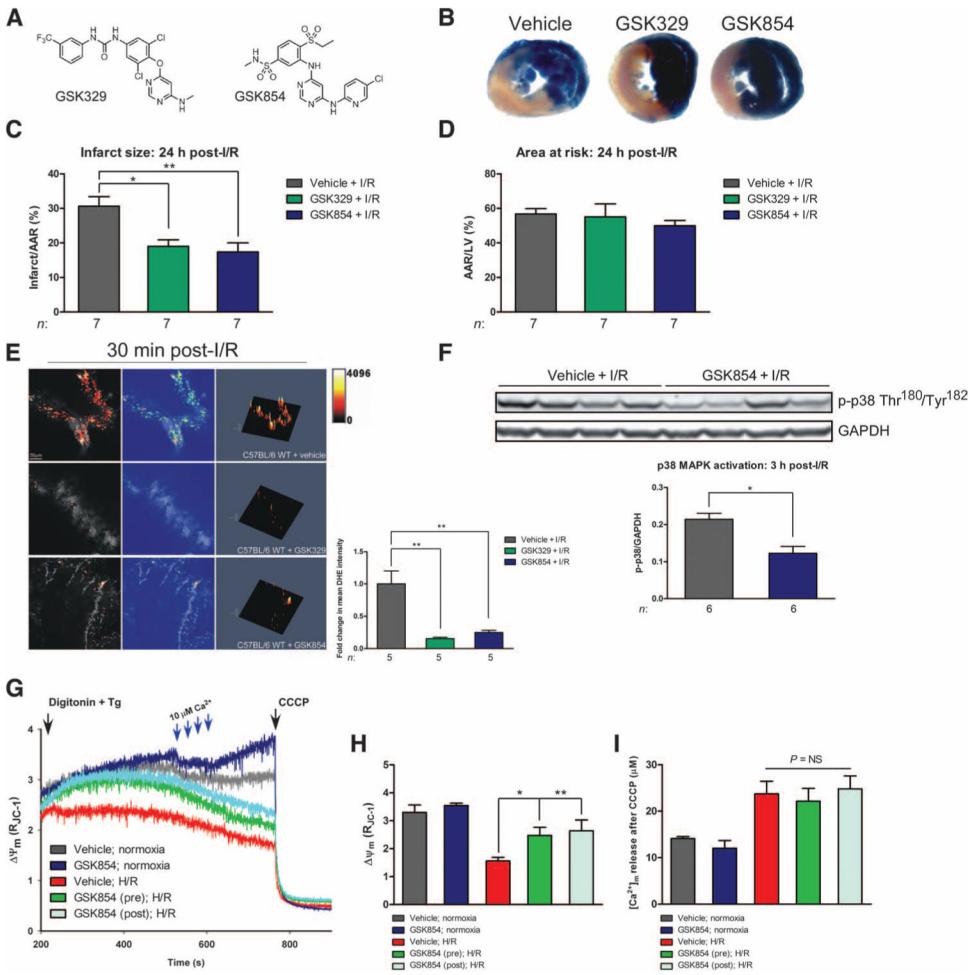

Fig. 6. Small-molecule TNNI3K inhibitors reduce infarct size and protect the heart after I/R

WT C57BL/6 mice were treated at reperfusion with vehicle [20% aqueous Cavitron + 5% dimethyl sulfoxide (DMSO)] or two small-molecule TNNI3K inhibitors. (**A**) Chemical structures of small-molecule inhibitors. (**B**) Representative LV sections from $n = 7$ animals per group, 24 hours after I/R. Dashed lines demarcate infarcted tissue. (**C** and **D**) Infarct sizes and AARs 24 hours after I/R. (**E**) Representative confocal micrographs from $n = 5$ animals per group of DHE-stained LV tissue. Quantification of superoxide levels (as fold change in mean DHE intensity versus vehicle treatment at 30 min after I/R) is shown below the representative images. (**F**) Immunoblots for p38 MAPK phosphorylation status in ischemic LV lysates 3 hours after I/R. GAPDH served as a loading control. Quantification is shown below. (**G**) Mitochondrial membrane potential ($\Delta\psi_m$) at baseline or in response to four pulses of 10 μM Ca^{2+} in WT C57BL/6 mouse myocytes subjected to hypoxia (1% O_2) for 2 hours, followed by reoxygenation for 30 min. Cells were treated with GSK854, immediately before hypoxia (Pre) or upon reoxygenation (Post). (**H** and **I**) Quantification of $\Delta\psi_m$ (H) and bath [Ca^{2+}] after CCCP (I), in response to four pulses of 10 μM Ca^{2+}, from $n = 3$ animals per group. All data are shown as means ± SEM. $^*P < 0.05$, $^{**}P < 0.01$ as determined by two-tailed Student's *t* test (F) or one-way ANOVA followed by Tukey's post hoc test (all others).

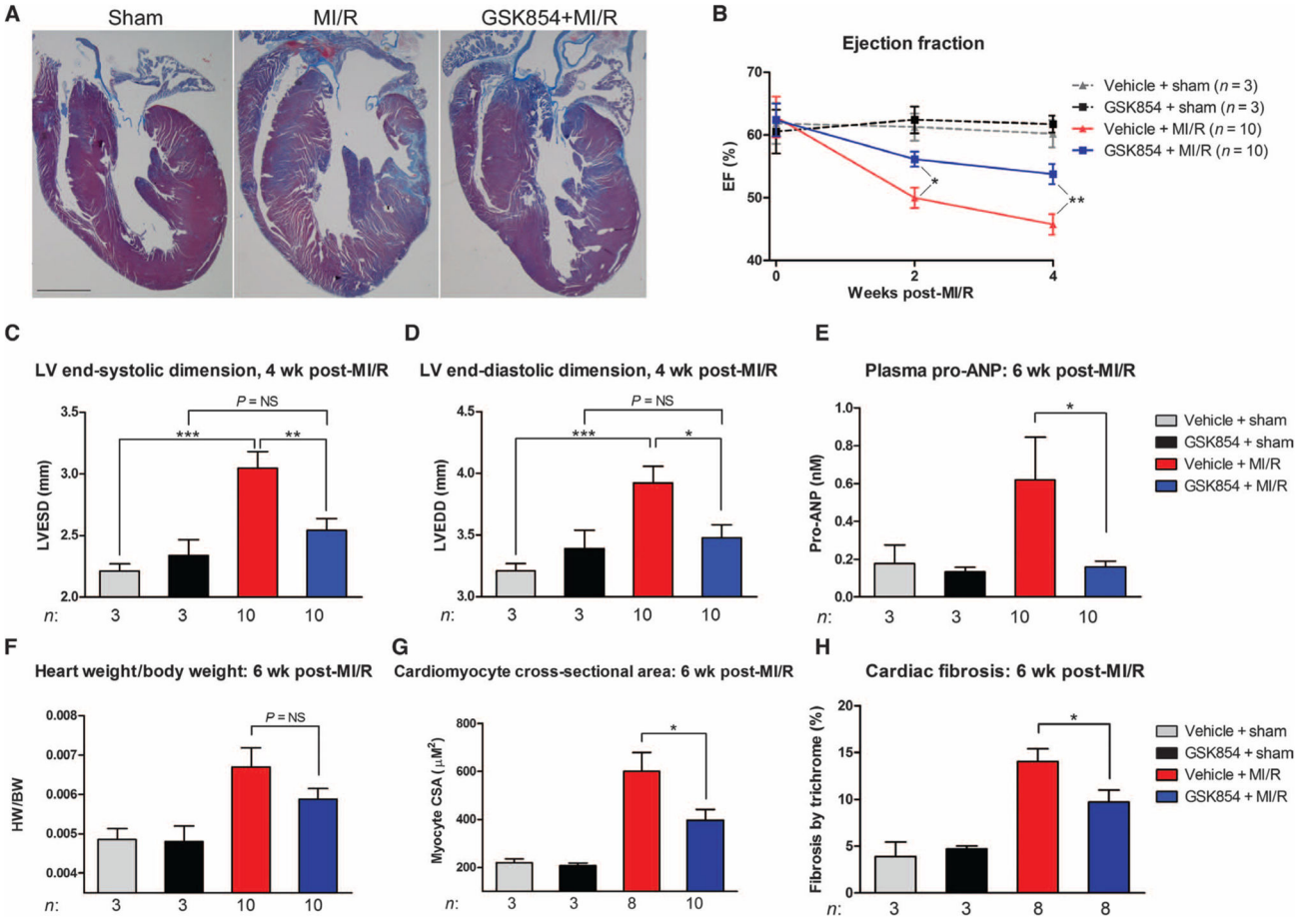

Fig. 7. TNNI3K inhibition reduces chronic LV dysfunction and limits progressive remodeling after MI/R

C57BL/6 mice were subjected to 40 min of LV ischemia. GSK854 (2.75 mg/kg intraperitoneally) was administered at reperfusion and at 6 hours after reperfusion. Animals were then placed on GSK854 (100 mg/kg; in chow) for 6 weeks. (**A**) Representative low-magnification images from $n = 3$ (sham groups) or $n = 10$ (MI/R groups) hearts stained with Masson's trichrome stain. Scale bar, 1 mm. (**B**) Ejection fraction (%EF) at 2 and 4 weeks after MI/R, measured by two-dimensionally directed M-mode echocardiography. (**C** and **D**) LV end-systolic dimension and LV end-diastolic dimension as measured by M-mode echocardiography 4 weeks after MI/R. (**E**) Plasma pro-ANP levels assessed by enzyme-linked immunosorbent assay in the various groups at 6 weeks after MI/R. (**F**) Heart weight/body weight ratios at 6 weeks after MI/R. (**G**) Cardiomyocyte cross-sectional area (CSA) in the above groups as measured from the LV of hematoxylin and eosin–stained sections. (**H**) Quantification of fibrosis for the hearts shown in (A). All data are shown as means ± SEM. $*P < 0.05$, $**P < 0.01$, $***P < 0.001$ as determined by one-way ANOVA followed by Tukey's post hoc test. NS, not significant.